TECHNICAL ARTICLE



Nanocarbon-Infused Metal Matrix Composites: A Review

WILSON RATIVA-PARADA¹ and SABRINA NILUFAR^{1,2}

1.—School of Mechanical, Aerospace, and Materials Engineering, Southern Illinois University, Carbondale, IL 62901, USA. 2.—e-mail: sabrina.nilufar@siu.edu

This paper presents an overview of the characteristics and advantages of carbon nanostructures as reinforcement in metal matrix composites. First, the main carbon nanostructures are summarized. Then, the most common and some new manufacturing methods for carbon—metal matrix composites are reviewed. The associated challenges regarding dispersion, interfacial bonding, and wettability during manufacturing are also discussed. The major properties of the carbon—metal matrix composites with aluminum, copper, titanium, magnesium, and nickel as base metals are summarized. Finally, the trends and future directions of nanocarbon-infused metal matrix composites are highlighted.

INTRODUCTION

Metals and their alloys are well known for their high strength, toughness, and elastic modulus. However, with the increasing demand for materials in automotive, airline/aerospace, defense, oil/ gas, sports, and electronics industries, a need for lighter materials with better physical and mechanical properties has been recognized. This quest has led to the development of metal matrix composites (MMCs). These materials are formed by a metallic base (usually Al, Cu, Mg, Ni, or Ti), and a reinforcement (commonly nitrides, metal oxides, carbon, and carbides).8 The reinforcement can be mainly particles or fibers,9 and it tends to improve the density, ¹⁰ and the mechanical ¹¹ and electrical properties ¹² of the base metal. An adequate reinforcement is required to have good mechanical and chemical compatibility with the metal matrix.¹ MMCs have excelled for having high hardness, thermal conductivity, tensile strength and ductility, corrosion resistance, and low thermal expansion coefficient compared with the base metals. 2,14,15 However, MMCs present limitations such as poor dispersion of the reinforcement,⁵ weak interfacial bonding, and poor wettability between the two components, 16 which have limited their performance and large-scale production.

In recent years, wettability has been treated through doping with carbide formers and surface modification, due to the physical bond and the large contact angle between metal and carbon. Magnesium can be used to increase the formation of carbides between metal alloys and carbon. Previtali et al. manufactured aluminum matrix composites with 1% of magnesium by stir casting to enhance the wettability between the metal matrix with silicon carbide (Fig. 1a, b) and boron carbide (Fig. 1c, d) and so avoid undesirable reactions. Similarly, Yang et al. utilized a coating of tungsten at the interface between graphite and a copper matrix to boost the thermal conductivity of the composite by more than 40% (Fig. 2a–c).

Interfacial bonding also plays an important role in the mechanical properties of MMCs. Interfacial bonding between the metal and the reinforcement can be improved by utilizing alloying, the addition of wetting materials, and heat treatments. 14,20,21 For instance, the usage of silicon carbide in carbon nanotube-aluminum matrix composites (CNT-Al MMCs), obtained by powder metallurgy, can reduce the reactivity between the aluminum and the carbon, hindering the formation of aluminum carbide (Al₄C₃), as shown in Fig. 3.²² Although interfacial bonding can help transfer loads from the matrix to the reinforcement and increase the mechanical properties of MMCs, the ductility of the matrix can also be affected by the characteristics of the interface region. Poor interfacial bonding has also been addressed by alternative synthesis

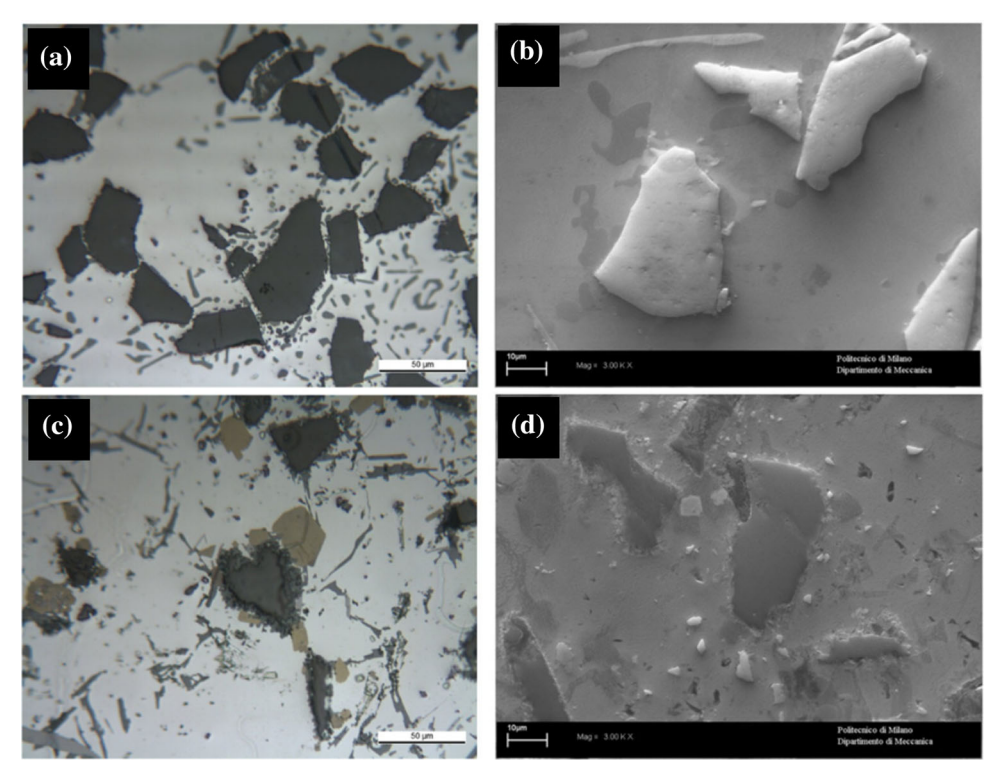


Fig. 1. Scanning electron micrographs of aluminum matrix composites reinforced with (a, b) SiC, and (c, d) B₄C using a liquid manufacturing process and magnesium as the carbide former. Reprinted with permission from Ref. 18.

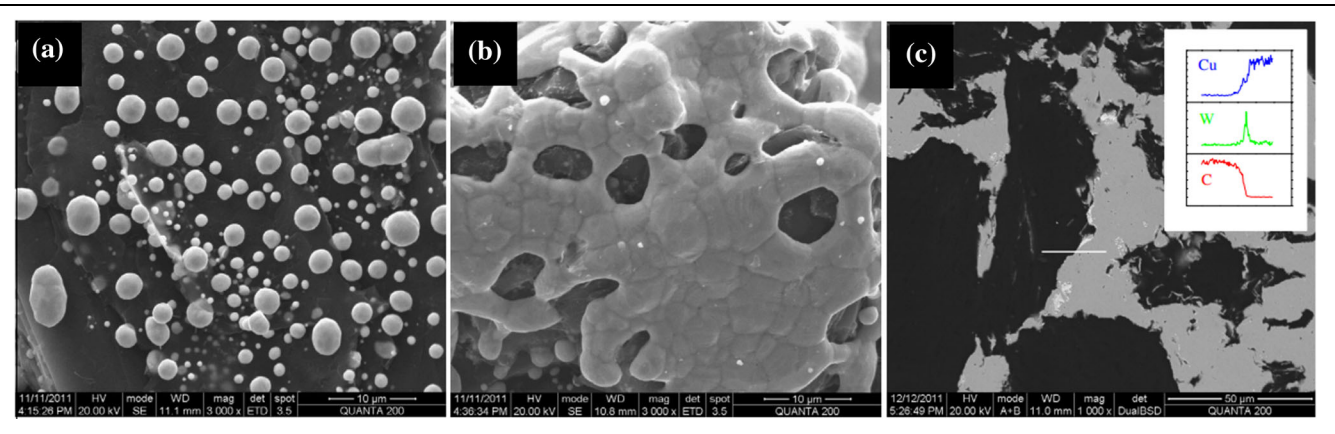


Fig. 2. Scanning electron micrographs of carbon nanotubes—copper matrix composites (a) before and (b, c) after a coating of the reinforcement with tungsten was performed to enhance the wettability between the carbon nanotubes and the copper. Reprinted with permission from Ref. 19.

methods, such as the electrocharge-assisted process, in which high electric energies are employed to ionize carbon and metal components, creating a covalent bonding between them. ²³

MMCs can develop chemical and physical bonding. In the chemical bond, a carbide interface between the two components of the composite is formed. This carbide formation can improve the mechanical properties.²⁴ However, in most cases, large amounts of carbide compounds degrade the mechanical properties of MMCs.^{25,26} Likewise, the physical bonding affects the surface roughness of the reinforcement and also any external wetting

agent or carbide former introduced to enhance the mechanisms of interaction between the base material and the reinforcement.²⁷

To reduce the lack of dispersion and agglomeration, Wang et al. synthesized carbon nanotube-copper matrix composites (CNT-Cu MMCs) by a combined electroless deposition and spark plasma sintering process. ²⁸ The CNT was activated through purification, oxidation, and sensitization, and was then reduced by electroless deposition and surface-coating with nano-copper (Cu-CNT). Cu-CNT powders and CNT powders were individually dissolved under sonication in anhydrous ethanol. The two

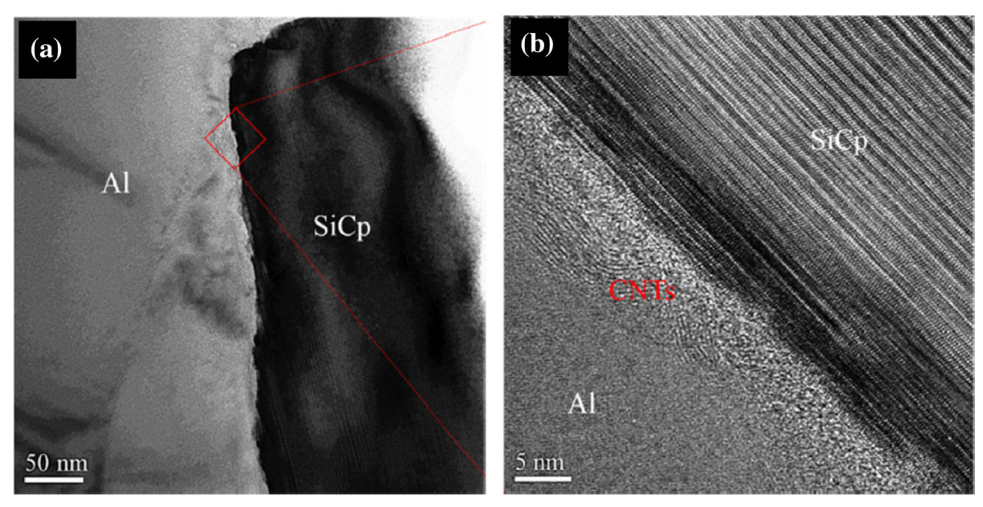


Fig. 3. Transmission electron micrographs (a) at 50 nm and (b) at 5 nm showing the effect of silicon carbide on the carbon aluminum interface. Reprinted with permission from Ref. 22.

parts were blended and mixed with polyethylene glycol, stirred for 2 h, filtered, and dried at 50°C for 24 h in a vacuum. The previous powders were later sintered by spark plasma at 700°C and 50 MPa for 5 min. The compositions obtained through this process presented higher compatibility between the two components, which was reflected in a better reinforcement distribution with low agglomeration. 28

Carbon MMCs follow at least one of the following four strengthening mechanisms: Orowan mechanism, thermal mismatch, Hall–Petch effect, and load transfer mechanism.²⁹ The Orowan mechanism states that the strength of the material will be enhanced by the movement restriction and stacking of dislocations around the reinforcement in the metal matrix. In the case of the thermal mismatch, since the coefficients of thermal expansion are different between the metal and the reinforcement, plastic deformations produced in the matrix will increase the density of dislocations during the cooling of the components. The Hall-Petch effect is a grain boundary mechanism where an impediment of dislocation movement within the matrix is prevented by changing the grain size.³⁰ Finally, the cohesion between the matrix and the nanocarbon contributes to boosting the transfer capacity of loads from the matrix to the stronger reinforcement material, increasing the strength of the composite.³¹

The increasing interest in the diverse carbon MMCs is reflected in the number of publications over the last decade, as shown in Fig. 4a. The predominant carbon reinforcements have been graphene and carbon nanotubes (Fig. 4b), due to their inherent characteristics, which are described below.

NANOCARBON ALLOTROPES

Carbon can form many different structures (Fig. 5) due to its unique sp² and sp³ hybridizations, ³³ which allow the formation of structures as soft as graphite and as hard as diamond. ³⁴ Diamond is stronger than graphite or any other carbon structure due to the covalent bond between the carbon atoms, in contrast with the weak van der Waals forces between the layers of the graphite sheets. ³⁵

Fullerene

Fullerene was discovered in 1985, a whole new research area was developed, and, subsequently, a great number of investigations into carbon fullerene-reinforced composite materials emerged.³⁶ The fullerene family consists of carbon molecules that can be formed in different shapes including hollow spheres, ellipsoids, or tubes. The different forms of carbon have their own specific names, such as buckyballs for hollow spheres, and carbon nanotubes (CNTs) for cylindrical shapes.³⁷

Carbon Nanotubes (CNTs)

In 1952, Radushkevich and Lukyanovich first observed and described CNTs. ³⁸ There are two types of CNTs: single-walled nanotubes (SWNTs) and multi-walled nanotubes (MWNTs). In recent years, both have been deployed as reinforcement for metallic matrices due to their excellent mechanical properties. ³⁹ In addition, MWNTs, which consists of multiple SWNTs wrapped around each other, were discovered accidentally by Iijima in 1991 when trying to formulate the C60 fullerene. ⁴⁰ Since then, CNTs have been extensively researched due to their excellent electrical, thermal, and mechanical properties, including a minimum of Young's modulus (1 TPa), extremely high conductivity (3000 W/mK), and non-corrosive properties to both acid and alkali

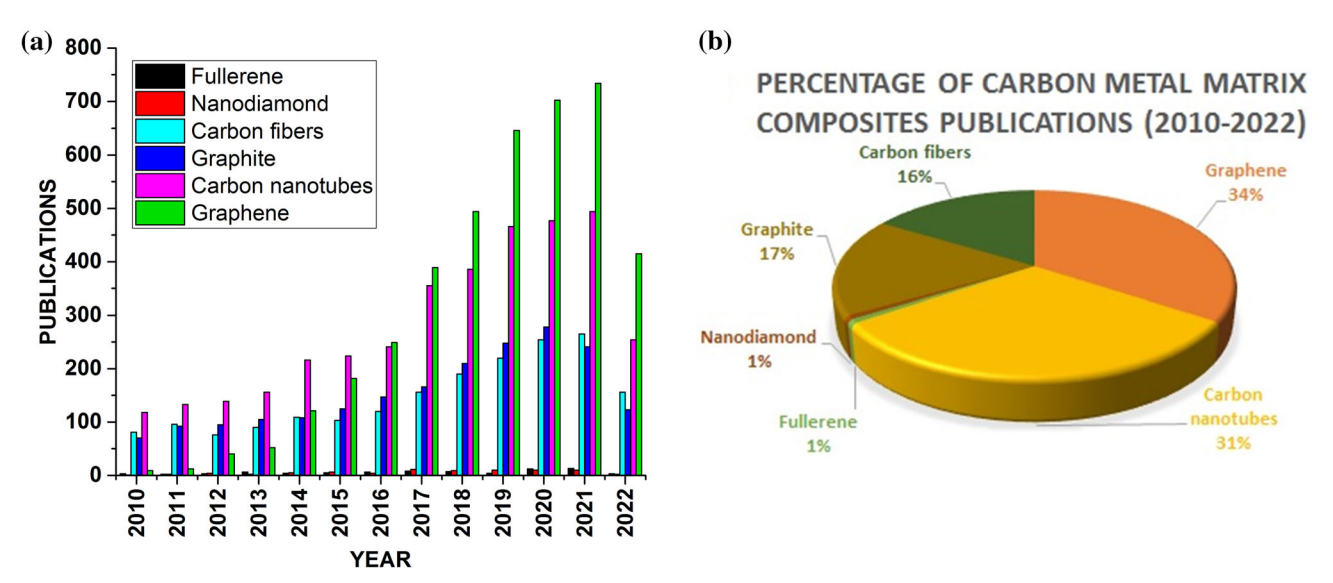


Fig. 4. (a) Number of publications on carbon metal matrix composites over the period 2010–2022, (b) predominant carbon structures employed in carbon metal matrix composites over the period 2010–2022. Data for these figures were collected from Ref. 32.

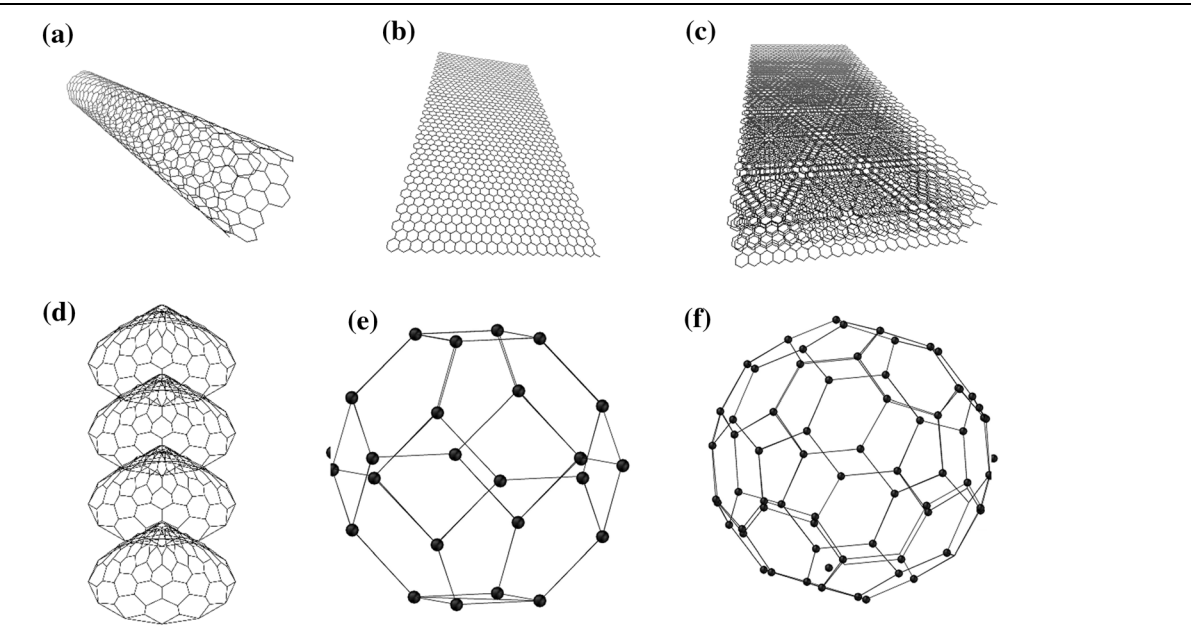


Fig. 5. Carbon allotropes: (a) carbon nanotubes, (b) graphene, (c) graphite, (d) nanofibers, (e) nanodiamond, and (f) fullerene.

media. 41–43 SWNTs can be compared to the single roll of a flat graphene sheet into a cylinder. The three major methods to synthesize CNTs are: laser vaporization, arc-discharge (above 1700°C), and chemical vapor decomposition (CVD). 38 The use of a combination of two metals, such as Co, Ni, Y, and Fe, has been favorable for the production of SWNTs, especially Co/Y and Ni/Y. 44 Moreover, CVD is the only non-batch-scale process that will not limit production capacities. CVD is also widely accepted these days, since this process allows the orientation, alignment, resizing, and purification of CNTs. 38

Carbon Nanofibers

The development of nanofibers started in the 1960s and has supported the subsequent development of nanotubes. Carbon nanofibers are characterized by presenting high mechanical properties, low densities, and low thermal expansion coefficients. They present a preferred orientation that facilitates their good mechanical, electrical, and thermal properties across the axis of the fiber. They are mainly produced from polyacrylonitrile through CVD and melt-spinning. The electrospinning method, usually employed to synthesize polymers, has also been adapted to obtain carbon

nanofibers. Inagaki et al. synthesized carbon nanofibers from polymers nanofibers obtained by electrospinning. Then, they carried out a carbonization process at 1000°C to obtain carbon nanofibers. 46

Graphene

Graphene was first synthesized in 2004, since then it has excelled in its physical, chemical, and mechanical properties, and has been demonstrated to be an alternative to CNTs due to a better dispersion into the metal matrix and good bonding interfaces. It consists of the sp² hybridized single atomic layer of carbon and has potential applications in catalysts, optics, and electronics. It is mainly produced by mechanical exfoliation and thermal decomposition of silicon carbide, CVD, and thermal reduction of graphite oxide.

Nanodiamond

Nanodiamond is characterized by presenting the sp³ hybridization and forming stable carbon aggregates at ambient temperature.⁵¹ It excels in having an excellent hardness, inertness, and optical and thermal properties.^{52,53} Techniques to process nanodiamond include detonation, CVD, and laser ablation. It has been used as reinforcement for ceramics, polymers, and metals in biomedical applications due to its low toxicity.⁵⁴

Graphite

Graphite is the most stable structure of carbon under ambient conditions, and is divided into crystal flakes, crystal lumps, and amorphous. ^{55,56} Graphite presents a hexagonal or rhombohedral layered structure forming 120° between carbon atoms with covalent bonding between the layers and weak van der Waals bonds perpendicular to the layers. ^{57,58} Due to its anisotropy, graphite presents good electrical and thermal conductivities across strong covalent bonds. ⁵⁹ Graphite is commonly used as an electrode conductor and solid lubricant. ⁴⁵ It is obtained by exfoliation, reduction, and deposition methods. ⁶⁰

SELECTED PROCESSING TECHNIQUES

Techniques to produce C-MMCs are divided into solid, liquid, and deposition. Powder metallurgy and friction stir processing are the most common solid methods. Liquid methods include stir casting and an electrocharge-assisted process. The most employed deposition methods are cold spray and plasma spraying. Some outstanding properties achieved through these techniques in MMCs are shown in Fig. 6 and Tables I and II.

The most common processing techniques employed to produce nanocarbon-infused MMCs are shown in Fig. 7. In addition, the characteristics of some selected carbon metal matrix composite-processing techniques are described below.

Stir Casting

Stir casting is an economic process that consists of melting the matrix metal by employing an induction or electric furnace and later adding particulate reinforcement to the molten material. The reinforcement is usually dispersed by mechanical stirring. Several strategies have been implemented to increase the efficiency of this method, such as centrifugal, squeeze, and pressure infiltration. In centrifugal casting, the molten material is transferred to a rotating mold, which is maintained at high pressure. In the squeeze casting process, the composite is poured into a die in which the material is then hydraulically pressed. In pressure infiltration, the molten matrix is injected at high pressure into a mold that contains the reinforcement.

Powder Metallurgy

Powder metallurgy is the most employed technique to fabricate carbon MMCs. The powder metallurgy method consists of an initial mixing of the raw material powders with a control agent9 through ball milling, 92 ultrasonication, 93 or both. 94 Ball milling involves the use of small balls, usually steel or zirconia.95 Some reports have found that higher velocities and larger times of mixing ensure better properties for the resulting composites. 96,97 The mixed powders are uniaxially compressed by using a wide range of forces. Compression can be made at room and high temperatures by following either hot pressing, 98 spark plasma sintering, 99 or deformation processing. 100 Room-temperature compression is followed by a sintering step up to 24 h. 101,102 Composites obtained by powder metallurgy are often subjected to post-treatment to improve their properties. Hot extrusion 103 and hot rolling¹⁰⁴ are some of the most common post-treatments for powder metallurgy-obtained carbon MMCs. It has been observed that the application of these secondary processing after the consolidation step assures an increase in the mechanical properties of the composites. 105 Some of the issues presented in this method include poor interfacial bonding due to low temperatures of consolidation, and poor dispersion of the reinforcement. 106

Cold Spraying and Plasma Spraying

C-MMCs have also been manufactured by cold spraying ¹⁰⁷ and plasma spraying. ¹⁰⁸ Cold spraying is performed at room temperature with supersonic speed and pressurized helium gas. ¹⁰⁹ On the other hand, plasma spraying melts the materials at atmospheric pressure with a thermal spraying source. The metal and the reinforcement are deposited in a molten or semi-molten state on the substrate. The cold spraying process presents some advantages over plasma spraying. They include no bulk particle melting due to the low temperature of the process, no requirement of electrical heating

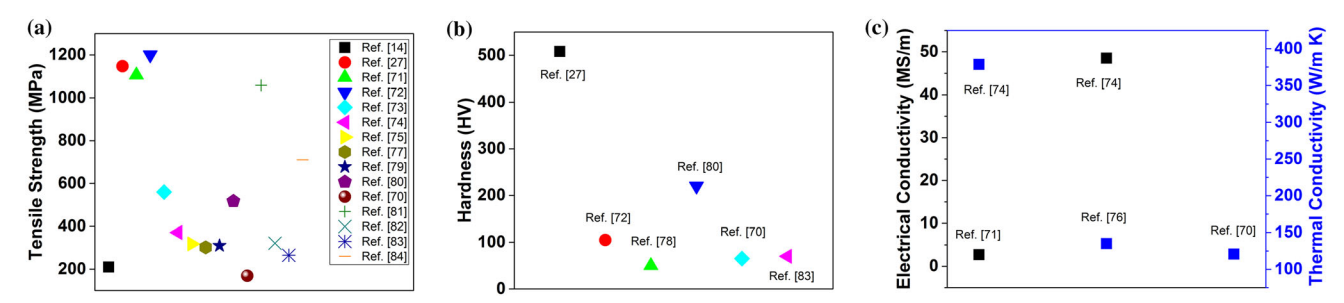


Fig. 6. Outstanding (a), tensile strength, (b) hardness, and (c) electrical and thermal conductivity of selected carbon-reinforced metal matrix composites.

equipment or fuel gases, high hardness, lack of stresses caused by temperature changes, and highly dense coatings with minimal effects created by oxidation and phase changes. However, cold spraying is a high-cost process due to the employment of inert gas and ductile binders for hard brittle materials. ¹¹⁰

Electrocharge-Assisted Process

This method was first introduced by Third Millennium Materials LLC, who devised a new method based on the combined use of an induction furnace and an electric arc system. In this manufacturing process, the base metal is melted in a conventional induction furnace while stirring. After adding carbon, the melted metal is subjected to an electric arc discharge, with the help of two graphite electrodes, to obtain the energy necessary to ionize the carbon. It is believed that this creates covalent bonding between the metal and the carbon ions. 65

Recently, variation of this method was implemented by Ma et al. This method, known as electrobeam melting, starts with mechanical mixing between powder carbon and powder metal, followed by drying in a vacuum environment, grinding, and pressing in pellets. Samples were introduced into the melting chamber, in which they are melted by applying a power of 8 kV and 1200 mA. The control of the position of the sample inside the chamber allows the samples to be stirred electromagnetically. Then, the molten material was cooled by using a vacuum. From scanning electron microscopy (SEM) images, the authors could identify the formation of carbon nanoribbons with a size ranging from 20 nm to 50 nm. Likewise, results from high resolution transmission electron microscopy (HRTEM) showed that the carbon nanoparticles were comprised of distorted graphite sheets. They further investigated the behavior of this 0.4 wt.% carbon-copper as a thin film. From the sample previously produced by electro-beam melting, they deposited layers approximately 18 nm thick on sodium carbide and glass substrates by electron beam evaporation. SEM characterization of the films showed that they were formed by graphitic carbon nanosheets into an interconnected carbon pathway, as well as by some parts of amorphous carbon. 66

Other efforts to manufacture C-MMCs based on the electrocharge-assisted process have been published recently. In 2020, Kareem et al. 111 synthesized Al with 3 wt.% of carbon by using a furnace and electric configuration constructed entirely in their laboratory. They employed aluminum wires and graphite powder as starting materials. Graphite was dried under vacuum at 250°C for 1 h and rolled in aluminum foils before being introduced into the molten aluminum, which was held at $850^{\circ}\text{C} \pm 5^{\circ}\text{C}$. A set of amperages, voltages, and current flow times were utilized to create the electric arc (170 A at 12 V and 24 V; 290 and 400 A at 36 V; 6, 8, and 16 min), and, therefore, determine the minimum values required for the electrocharge-assisted process to occur. Other details of the manufacturing process include the employing of a blender to stir the molten metal and the subsequent pouring of the molten aluminum into previously lubricated and heated steel molds. The final step was to allow the poured material to cool in an air atmosphere. They concluded that applying 170 A and 12 V was enough for carbon ionization to take place, and, more importantly, that the composition obtained under these conditions presented higher values of conductivity and hardness, as well as a lower density. 111

DIFFERENT METAL MATRIX COMPOSITES

The most common metals used for MMCs are mentioned here. A review of the most recent compositions with outstanding properties, as well as the current trends for manufacturing techniques of each metal matrix, is discussed.

Aluminum Matrix Composite

The main objective to introduce carbon to aluminum is to enhance the mechanical properties, which has been reached up to a point, but there still exists the problem of decreased ductility. Carbonaluminum matrix composites (Al-C MMCs) have drawn attention due to their high tensile strength and modulus, low density, high stiffness, and wide potential applications. High stiffness and wide potential applications of MWCNT-reinforced aluminum MMCs fabricated by a powder metallurgy

	Table I. Selected	processing techniques	for manufacturing	nanocarbon-infused	metal matrix composite
--	-------------------	-----------------------	-------------------	--------------------	------------------------

Process	Description	Advantages	Disadvantages	Reference
Cold spraying	Particles are accelerated at low temperature to a substrate. Deposited particles are plastically deformed and create a bond with the substrate	High homogeneous distribution of the particles Phase transformations are avoided	Plastic deformation involved in the process creates agglomeration	61, 62
Plasma spraying	Molten particles are projected to the substrate	Highly crystalline coatings	High cost	63, 64
Electrocharge- assisted pro- cess	Reinforcement particles are added to the molten matrix The bath is subjected to an arc discharge at high amperages	Strong interfacial bonding Superior carbon solubility	Lower reinforcement content than the calcu- lated Inhomogeneous dispersion of the reinforcement	65, 66
Stir casting	Reinforcement is added to the molten matrix while mechanical stirring	Low cost High compressive strength	Interfacial reaction be- tween matrix and rein- forcement Aggregation of reinforcement Undesirable chemical reactions	67, 68
Powder metallurgy	Mixing of matrix and reinforcement by ball milling Compaction and sintering through hot pressing and spark plasma sintering	Low formation of by-products Synthesis of a wide range of compositions	Reduction in the aspect ratio of the carbon rein- forcement Inhomogeneous dispersion of the reinforcement	69, 70

route. A uniform distribution of the carbon nanotubes with a composition of 0.6 wt.% was observed. From the tensile test, it was found that the carbon nanotubes started to elongate and to act as ligaments to avoid the propagation of cracks, and, more importantly, a strengthening mechanism was also presented due to a load transfer effect across the nanotube walls. 69

Aluminum matrix composites have also been reinforced with graphene nanoplatelets. Alam et al. fabricated graphene nanoplatelet-aluminum matrix composites (1-5 wt.%) by employing a powder metallurgy method. Their results showed an increase in the homogeneous distribution, wear resistance, and hardness at low doping levels (< 3 wt.%) due to a later formation of Al_4C_3 . 115 Carbon nanodiamond has also been employed as a reinforcement in aluminum matrix composites. Woo et al. utilized high-energy ball milling and low pressure cold spray techniques to produce an aluminum matrix composite with a reinforcement of 10 wt.% nanodiamond. Their synthesis process included the mixing of both aluminum and nanodiamond powders in a ball mill for between 0.5 h and 3 h, and then a heat treatment of 24 h at 420 °C. An important finding was that nanodiamond affects the behavior of the powders in the milling process, by reducing the grain size due to its brittleness. They found that the coating had superior mechanical

properties (elastic modulus = 98.3 GPa, hardness 3.27 GPa) due to strain hardening and grain reinforcement. Raman spectra also revealed the presence of Al_4C_3 formed during the milling process.⁶¹

Chen et al. studied the coefficient of friction and mechanical properties of Al-CNT MMCs obtained by cold spraying. Their results showed that the indentation depths decreased and the elastic modulus and hardness increased as the reinforcement increased between 0.5 wt.% and 1 wt.%. 116 They concluded that the cold-sprayed Al-CNT MMCs have higher elastic strength and hardness than the cold-sprayed Al-CNT MMCs.On the other hand, the coefficient of friction of the composite did not present any change with the addition of CNT. 116 In turn, plasma spraying produces purer, denser, and stronger although deposits, requires complex equipment. 117,11

Another attempt to improve the mechanical properties without sacrificing the ductility of the CNT–aluminium MMCs has been through the modification of their bonding conditions. Chen et al. implemented a series of synthesis techniques including ball milling of the Al powders, mechanical solution coating to incorporate CNTs (1 wt.%), spark plasma sintering at 526°C, 576°C, and 626°C, and a final hot extrusion step using a pressure of 30 MPa. The best mechanical properties were achieved at the higher sintering temperature, showing that high

Table II. Characteristics of carbon-reinforced metal matrix composites as mentioned in Fig. 6

Composition	Reinforcement	Synthesis method	Reference
1.3 wt.% of C in Mg	Carbon nanotubes	Disintegrated melt deposition	14
1 wt.% of C in Ni	Graphene	Selective laser melting	27
0.4 wt.% C in Ti	MWCNT	Spark plasma sintering	71
1 wt.% of C in Al	Graphene	Spark plasma sintering	72
0.5 wt.% of C in Al	Few-layered graphene	Powder metallurgy	7 3
5 wt.% of C in Cu	MWCNT	Electroless plating, and die-stretching	74
2.0 wt.% C in Cu	3D graphene-like network	In situ processing	75
2 wt.% of C in Al	Cu coated carbon nanofibers	Rheocasting and extrusion	76
15 vol.% of C in Cu	Super-aligned carbon nanotubes	Electrodeposition	77
5 vol.% of C in Cu	Carbon nanotubes	Vacuum sintering method	7 8
0.6 wt.% of C in Cu	Graphene	Molecular-level mixing and SPS	7 9
0.75 wt.% of C in Ni	Carbon nanotubes	Spark plasma sintering	80
1.0 vol.% of C in Mg	Carbon fibers	Powder metallurgy	70
0.5 wt.% of C in Ti	Graphene	Powder metallurgy	81
1.0 vol.% of C in Mg	Carbon nanotubes	Chemical synthesis and hot extrusion	82
4.0 wt.% of C in Mg	Carbon nanotubes	Powder metallurgy	83
6 vol.% of C in Ni	Carbon nanotubes	Molecular-level mixing and SPS	84

temperature is the cause of better ductility and increased diffusion of the atoms in the CNT-Al interface. The CNT-Al interface was also investigated by Zhou et al. They observed that the better the CNTs are dispersed into the metal matrix, the more stable the C-Al interfaces that are formed. They also noted that a controlled formation of ${\rm Al}_4{\rm C}_3$ was useful to increase the load transfer strengthening due to the covalent bonding between the CNTs and the aluminum carbide. 120

Hanizam et al. utilized the stir-casting method to fabricate CNT-aluminum alloy matrix composites. Magnesium pellets were used as a wettability agent. Aluminum allov was melted at 700°C in an induction furnace, then the CNT powders and magnesium were mixed, wrapped in aluminum foils, and added to the molten aluminum alloy. The batch was stirred at 200 rpm for up to 10 min and poured into a mold. Then, the samples were subjected to the forming process, which consisted of transferring the samples to a pneumatic cylinder placed within the heating coil of the furnace. The system was heated at 580°C and a forging load of 5 tons. SEM images showed a homogeneous CNT distribution and their presence in the aluminum alloy grain boundaries. Also, they concluded that longer stirring times produced materials with better mechanical properties. The amount of CNTs also influenced the mechanical properties of the composites, for example, the composition with 0.5 wt.% of CNTs was the one that obtained the highest hardness. 121 Isaza et al. reinforced ASTM-100 aluminum with MWCNTs through a sandwich technique. The MWCNTs were dissolved in a solution of polyvinyl alcohol and distilled water. Then, the resulting solution was stirred for 1 h, sonicated at 40–60 kJ, and cured for 8 days at room temperature. This technique allowed them to obtain composites with excellent tensile strength and elastic modulus due to an excellent dispersion and alignment of the MWCNTs within the metal matrix. 122

Copper Matrix Composite

The main objective to introduce carbon to copper is to decrease the overall density while increasing the mechanical and thermal properties for lightweight and heat sink applications. 123,124 One of the advantages of C-Cu MMCs is the small formation of carbides; however, wettability between Cu and C is still a challenge. Likewise, carbon-copper MMCs (C-Cu MMCs) present superior thermal conductivity ($\sim 3000 \text{ W/mK}$) compared to copper ($\sim 400 \text{ W/mK}$) mK). 125 Chu et al. obtained C-Cu MMCs by using spark plasma sintering (SPS). They found that the CNT reinforcement tended to form clusters in the metal matrix above 15 vol.%. Dong et al. measured the hardness and coefficient of friction of C-Cu MMCs by employing Ni-coated CNTs as reinforcement. The hardness increased up to 12 wt.% of CNTs, and the coefficient of friction decreased by up to 15 wt.% of reinforcement due to higher porosity and poor fracture propagation. ¹²⁶ In addition, Cha et al. found that CNTs are the most efficient compared to carbide reinforcements such as SiC. Yield strength and Young's modulus increased by up to 8 times by using between 5 vol.% and 10 vol.% of CNTs in C-Cu MMCs. 127 In another work, Chen et al. synthesized super-aligned C-Cu MMC films by electrodeposition. The procedure consisted of depositing CNT films on Cu layers previously obtained from an electroplated solution of copper sulfate, glucose, and sulfuric acid, employing different deposition times and volume fractions of carbon. They reached a high strength (302 MPa) without

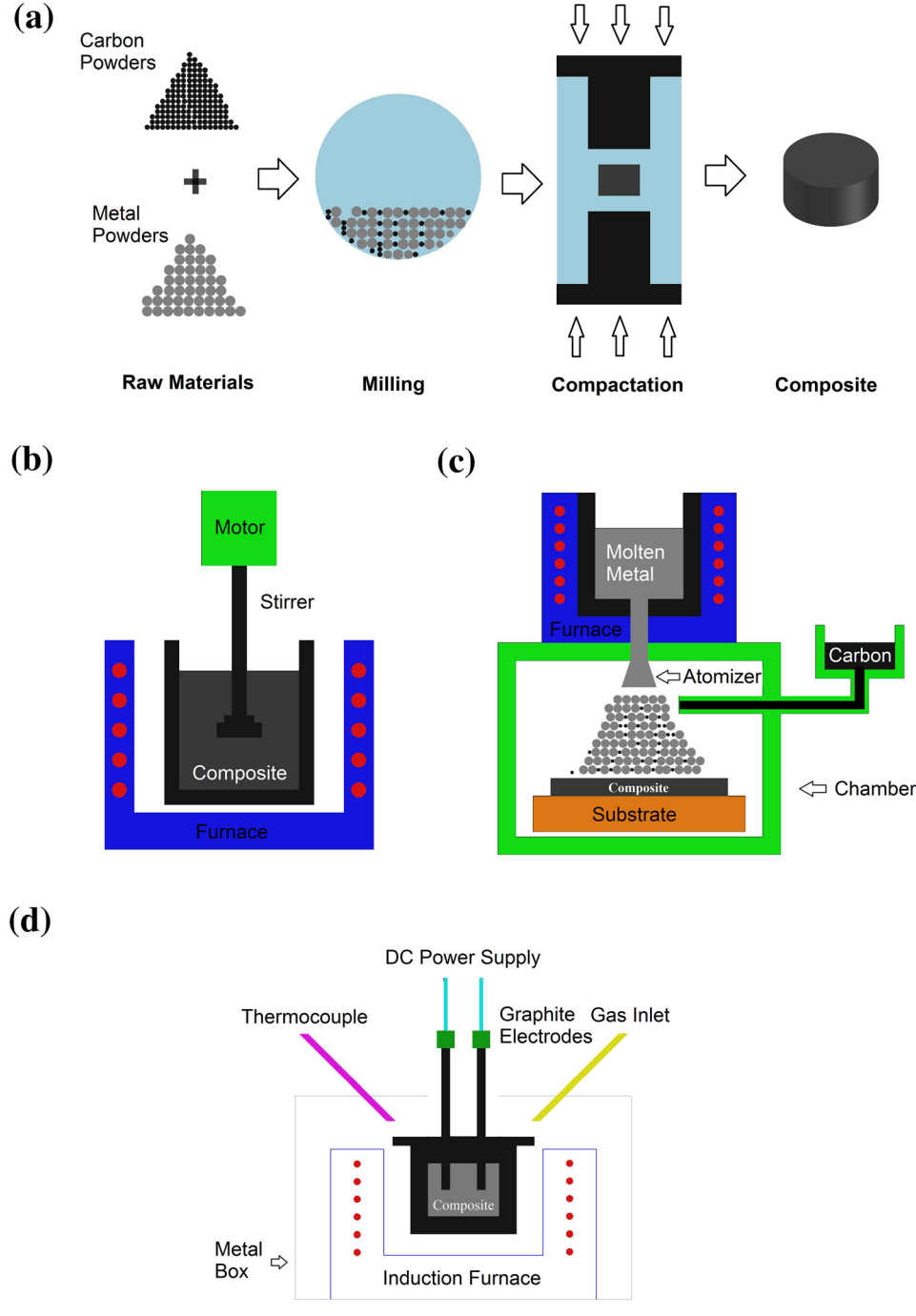


Fig. 7. (a) Powder metallurgy, (b) stir casting, (c) spray coating, and (d) electrocharge-assisted methods.

sacrificing ductility, which showed an outstanding value of 11.5%. ⁷⁷

New methods such as a 3D carbon network have recently been implemented to manufacture C-Cu MMCs. This method consists of an initial solution of Cu powders, ethanol, water, and sucrose, which was sonicated and heated at 75°C until evaporating and dried at 80°C for 4 h. The resulting material was introduced into a quartz tube and heated at 800°C

under Ar and H₂ atmosphere for 10 min. ¹²⁸ After employing the above methodology, Zhang et al. obtained graphene–copper matrix composites in which the thermal stress generated by the matrix and the reinforcement allow the creation of a regular 3D graphene network. This network is responsible for the exceptional mechanical and physical properties of this composite. ¹²⁸ Zhang et al. manufactured 5 vol.% graphene and graphene

oxide-reinforced copper matrix composites by a combined catalytic reaction—spark plasma sintering method. Graphene also results in a better reinforcement to copper matrix composites than graphene oxide because the presence of graphene oxide can facilitate the formation of copper oxides. This was attributed to the differences in the interfaces of the two compositions, since the graphene—copper interface was regular and without any contaminant, while the graphene—oxide interface appeared much more complex because of the presence of additional phases such as copper oxide and amorphous carbon. 129

Electrodeposition is a common method to manufacture nanodiamond-copper matrix composites, but a poor understanding of the carbon-metal interface has limited its implementation. Cho et al. utilized this technique to obtain different samples of this composite with 68 wt.%. They found that the thermal conductivity decreased at a small reinforcement size, which was ascribed to an increase in the electrical current density from the electrodeposition step. 130 Aligned CNTs were used as reinforcement for copper matrix composites by Zhao et al. They measured their performance concerning reinforcement dispersion and distribution, density, and interfacial interactions between the two components. SWCNTs were electroless-plated with Cu and Ni and dried in a vacuum for 3 h. The components were later mechanically stirred by sonication and dried again for 2 h at 40°C. The resulting powders were compacted at 50 MPa and sintered at 950°C for 120 min in an Ar atmosphere. SEM images showed a homogeneous distribution of the SWCNTs and a preferential alignment along the stretch direction, which led to the formation of an anisotropic composite.

In 2017, Zhang et al. manufactured graphenecopper matrix composites in a novel way. First, they dissolved copper (II) nitrate trihydrate, glucose, and sodium chloride in water while stirring. Then, the solution was placed at - 20°C until a dry gel was obtained. The resulting precursor was calcined at 750°C under an H₂ atmosphere for 2 h. The remaining sodium chloride was cleaned with deionized water. The graphene content in this material was 26.8 wt.%. The powders were impregnated with copper powder by an impregnation-reduction method. The final composition was placed into a graphite mold and hot-pressed sintered for 1 h in a vacuum at 800°C and 50 MPa. Their results showed the formation of a discontinuous graphene network sheet with strong interfacial bonding and high ductility due to the anchor and the high number of nucleation sites between graphene and cooper within the two synthesis steps. 75 The 3D graphene network sheet reinforcement was also explored by Zhang et al. by employing a powder metallurgy method. Cu powders were added to a solution of sucrose, ethanol, and water, and sonicated for 20 min at 75°C. The dry material (80°C for 4 h)

was transferred to a CVD quartz tube, which was heated at 800° C for 10 min in an Ar and H_2 atmosphere. The composite was placed in a graphite mold, pressed at 50 MPa, and heated at 800° C for 1 h. The thermal stress created due to the difference in the coefficient of linear thermal expansion of copper and graphene produced a welding process between the matrix and C-Cu MMCs reinforcement layers, which favored the strengthened interfacial bonding. 128

Nickel Matrix Composite

Nickel MMCs (C-Ni MMCs) have been studied as coatings in recent years. 131,132 Borkar et al. have carried out experiments using pulsed electrodeposition to manufacture Ni-C MMC coatings. CNTs were pretreated with nitric acid to unbundle them for homogeneous distribution inside the matrix. SEM was taken for the Ni and Ni-CNT MMC coatings. The Ni-CNT MMC coatings (9 μ m) are about half the Ni coatings (19 μ m) due to the restriction of Ni columnar growth by the CNTs. The experiment also showed that the microhardness of the Ni-CNT MMCs was more than 1.8 times higher than that of the unreinforced metal. This result also has proved the Hall-Petch and Orowan mechanisms to be the cause of the strengthening. 133 Carpenter et al. did similar testing and compared Ni, Ni-CNT MMCs with 1.6 vol.% and 3.7 vol.% for their wear behavior. The results are similar to those of Borkar et al. in that the wear resistance increased as the CNT reinforcement increased; although the wear rate started to flatten after 3.7 vol.% CNTs. 134 Yamanaka et al. studied the thermal conductivity and electrical conductivity of Ni-CNT MMCs by manufacturing Ni-CNT MMCs by SPS by varying the sintering temperature and volume fraction of the CNTs. Both the thermal conductivity and electrical conductivity of Ni-CNT MMCs with 1 vol.% CNT had their highest value at 873 K. 135

Some works have compared the properties of Ni and Ni-CNT MMCs. For example, there have been studies on wear resistance, ^{136,137} and on electron transport and electrocatalytic properties. 138 Likewise, Sun et al. studied the mechanical strength of carbon-nickel nanocomposites using SWNTs and MWNTs, ¹³⁸ and Jeng et al. nanotribologically characterized Ni-CNT MMCs. 139 In addition, Sahoo et al. have extensively investigated Ni-CNT MMCs with electroless plating methods to evaluate the hardness and wear properties of Ni-CNT MMCs. An electrodeposition technique has been employed to obtain carbon-reinforced nickel matrix composites from both activated carbon and 50-μm metal particles. 141 Carbon nanotube-nickel-reinforced matrix composites were synthesized by SPS with mass fractions between 0.25 wt.% and 1 wt.%. After the synthesis, part of the carbonaceous material was transformed into another morphology due to the pulsed current field involved in the sintering

step. The composition of 0.75 wt.% increased both the hardness and the ductility of the composite compared with that of nickel.⁸⁰

Nanodiamond has also been utilized as a reinforcement for nickel matrix composites. Suarez et al. studied transformations of nanodiamond structures at high temperatures. Raman spectroscopy results showed that the ratio sp³/sp² depends on the annealing temperature, being larger in the presence of sp² at higher temperatures of heat treatment. The powder metallurgy method has also been employed to fabricate graphene-nickel MMCs with 1 wt.%. The tribological performance of this kind of composite was evaluated by Lei et al., and XPS and Raman characterization showed that graphene increased the wear resistance of the composite by a transformation of the graphene into amorphous carbon and polymeric material due to the friction process. 143 Aristizabal et al. obtained CNT-nickel matrix composites by utilizing a plastic deformation process. They employed a colloidal technique to mix Ni and CNT powders, which were pressed at 990 MPa, sintered in a vacuum for 3 h at 900 °C, and subjected to high pressure torsion at 2 rpm, 4 GPa, and different turns (1,4, 10, 20). The high-pressure torsion generated grain refinement and hardening phenomena at high CNT contents due to an increase in screw dislocations. 144 Furthermore, experiments with other processes for other applications have been made, including Nicoated SWNTs used for lightning-strike protection, 145 materials for supercapacitors, 146 hydrogen storage, ¹⁴⁷ LCD backlights, ¹⁴⁸ direct methanol fuel cells, ¹⁴⁹ nanocomposite films for electrical contact applications, 150 and amperometric and potentiometric field-effect bio-chemical sensors. 151

Magnesium Matrix Composites

The incorporation of carbon structures in magnesium matrices seeks to enhance corrosion resistance and mechanical strength at room and high temperatures. 152 Hou et al. studied 1.5 vol. % carbon fibermagnesium matrix composites fabricated by powder metallurgy. Some carbon fibers were pretreated by nickel plating at 65 °C for 5 min in solutions with different pH values. X-ray diffraction (XRD) characterization of the coated samples showed the formation of Ni_3P and Mg_2Ni phases due to the presence of nickel, unlike the non-coated samples, in which none of these phases were present. Ni₃P and Mg₂Ni favored the interfacial wettability of the composites by creating a string combination between the carbon fibers and magnesium. The hardness of pure magnesium increased by more than 80% in the nickel-plated composite sample with 1.0 vol.%.⁷⁰

Xiang et al. synthesized magnesium matrix composites with graphene nanoplatelets as reinforcement (between 0.7 wt.% and 1.6 wt.%) by employing a novel method for carbon incorporation.

Commercial graphene nanoplatelets were dispersed in a surfactant and exfoliated ultrasonically. Magnesium and a solution of polyvinyl alcohol were mixed and stirred for 1 h. This semi-product was mixed with exfoliated graphene nanoplatelets and heated until reaching water evaporation. The resulting product consisted of polyvinyl alcoholmodified magnesium coated with graphene nanoplatelets. The final step consisted of adding the above product into a melted alloy of magnesium and zinc. The mechanical properties of the material increased as the concentration of the reinforcement increased, and they were higher than those of the untreated alloy due to reduced grain size and a load transfer effect. ¹⁵³

Nanofiber-reinforced magnesium matrix composites were obtained by Abdo et al. They used powder metallurgy and 1 wt.%, 3 wt.%, 5 wt.%, and 10 wt.% of carbon reinforcement. Consolidation of the bulk material was reached by high-frequency induction heat sintering. The introduction of carbon fibers into the magnesium matrix reduced the strength of the composite after using more than 1 wt.%. They concluded that reaching strong interfacial adhesion between the magnesium and carbon fibers increased the mechanical properties of the composite. 154 A CNT- reinforced magnesium matrix composite was manufactured through powder metallurgy with CNT surface modification. First, tetrahydrofuran and CNT were sonicated for 30 min, then Li powders, MgCl₂, and naphthalene were added to the solution, which was stirred for 24 h at room temperature. The resulting product was filtered, washed with ethanol, and dried in a vacuum at 70 °C for 3 h. Finally, the composite was cold-pressed at 500 MPa, and sintered for 1 h at 500°C. A later hot-compression step (700 MPa, 380°C) was also carried out. SEM images revealed the formation of crystal Mg nuclei in the form of a layer on the CNT walls. They concluded that the initial atomic level mixing of Mg and carbon produced in the initial step of the synthesis generated an enhanced interfacial bonding and wettability between the components.83

Titanium Matrix Composite

Carbon-titanium matrix composites (Ti-C MMCs) have been the main focus of study for their corrosion resistance, high tensile strength, light weight, and toughness at extremely high temperatures. Although Ti has excellent mechanical properties and the versatility of its uses has included environmental usage, the high cost of elemental titanium has limited it to mostly military applications. The Ti-C MMCs manufacturing processes include power metallurgy, mechanical rubbing, and a wet chemical process. Kondoh et al. manufactured Ti-CNT MMCs using CNT prepared with a zwitterionic surfactant, followed by SPS and hot extrusion. They evaluated the tensile strength and the hardness of

pure Ti-CNT MMCs and Ti-CNT MMCs with 0.18 wt.%, 0.24 wt.%, and 0.35 wt.% CNT additions. Although TiC was formed in this process, it was evenly distributed among the composite and no primary particle boundaries were formed, which would have been detrimental to the mechanical properties of the Ti-CNT MMCs. SEM micrographs also showed good wetting among the CNTs and Ti. In addition, an improvement in all the mechanical properties, including tensile strength, yield strength, and hardness, was shown. ¹⁵⁷

In similar experiments, Melendez et al. used power metallurgy to obtain Ti-CNT MMCs and MMCs titanium-nanodiamond (ND) (Ti-ND MMCs). They tested several percentage volumes of CNT (0.6 wt.% or 1.8 vol.%) and ND (1.4 wt.% or 1.8 vol.%) and compared the different results with different processing conditions. Hardness, flexural properties, and densities were measured with hotpressing consolidation temperatures from 900°C to 1300°C, and heat treatment temperatures from 1100°C to 1400°C. SEM and XRD were used to observe the reaction between Ti and the nanocarbon reinforcements. Moreover, the density for both the Ti-CNT MMCs and Ti-ND-MMCs increased dramatically as hot pressing and heat treatment temperatures increased. A higher hardness for both Ti-CNT MMCs and Ti-ND MMCs was significantly found over pure Ti as the hot pressing temperature increased. Furthermore, both ND and CNT were distributed more evenly when high-temperature heat treatment was used. TiC was only present in Ti-ND MMCs with high-temperature heat treatment, but not in Ti-CNT MMCs. Similar to aluminum, the TiC phase can cause the degradation of the Ti-CNT MMCs and Ti-ND MMCs. On the other hand, the flexural strength was better for the lowest hot pressing temperature of 900°C at 1473 MPa compared to 400 MPa for pure titanium. The flexural strength started to decrease at elevated hotpressing and heat-treatment temperatures. In the same way, after heat treatment, the difference between the Ti-CNT MMCs and Ti-ND MMCs was minimal. 158 In conclusion, the addition of up to 0.35% CNT improved the tensile strength, yield strength, and hardness, but failed to enhance the elongation percentage. Melendez et al. also proved that, with the same volume percentage, ND serves as a better candidate than CNT to reinforce titanium. Furthermore, they demonstrated that the heat treatment increased the hardness of the material but decreased the flexural strength for both the CNT and ND additions to Ti MMCs.

Ti-CNT MMCs were also evaluated as cold cathode coatings for flat panels. He et al. studied the field-emission properties of ${\rm TiO_2}$, where CNT can improve the uniformity and stability of vacuum electronic devices. The studies were carried out by using mechanical rubbing. Property improvement started at 7–10 wt.% CNT addition by lowering the turn-on field. 159 Furthermore, Lv et al. carried out a

similar study on Ti-CNT MMCs thin coatings on ${\rm Al_2O_3}$ substrates using a different processing technique to improve the cold cathodes on flat panel TVs and drew the same conclusion as He et al. ¹⁶⁰. Munir et al. used high-energy ball milling to obtain MWNCT-titanium matrix composites in a two-batch process. In the first batch, Ti powders were mixed with 5 wt.% between 1 h and 4 h at 200 rpm. Then 0.5 wt.% stearic acid was added to favor the fracture of the mixed powders on cold welding. Through TEM and Raman characterizations, they discovered the in situ formation of a TiC layer around the MWNCTs with high-energy ball milling, which increased the mechanical properties. ⁹⁶

CONCLUSION AND FUTURE DIRECTIONS

Several issues remain open for the manufacturing of nanocarbon-reinforced MMCs. There are fabrication challenges for the carbonaceous reinforcements involving the distribution into the metal matrix due to their large specific area/weight ratio. The nonhomogeneous particle dispersion and interfacial bonding issues are the main disadvantages of using the present manufacturing techniques. In addition, the challenges include distributing carbon uniformly throughout the matrix, especially when high concentration processes are being deployed, due to van der Waals forces. Other disadvantages include the difficulties in manufacturing carbon structures with uniform lengths and diameters, porosity, and bonding, which can also affect the thermal conductivity, microhardness, and Young's modulus of the C-MMCs, making the transference of the applied load in the interfacial bonding between metal and reinforcement difficult. Another relevant issue involves the tribological properties and fundamentals for mechanical design, which require further nanoscale and macroscale studies on their correlation with the reinforcement in C-MMCs.

Regarding improvement possibilities, perfecting of the distribution, size reduction, and partial elimination of undesirable compounds, such as the elimination of Al₄C₃ in aluminum matrices, dispersing of TiC in titanium matrices, and the formation of SiC compounds in copper matrices with Si-coated CNTs can be mentioned in the first place. Likewise, better bonding between carbon nanostructures and matrices by using wetting materials and different hot-pressing techniques may prevent the formation of undesirable compounds, which decreases the mechanical properties of the composites. Large chunks of brittle carbide formation should be prevented in the matrix, as they cause premature failure. Some metals, such as magnesium, do not easily bond with carbon, hence carbides need to be formed using some other chemical agents such as Si. These intermediate agents can serve two purposes. Firstly, to coat the carbon nanostructures to avoid

self-clustering, and secondly, to act as an intermediate component for the bonding between metal and carbon.

In the same way, critical carbon cluster size fractions should be determined, which may lead to an increase in the macro-wear resistance of the coatings and the reinforcement dispersion to maintain nanoscale properties at macroscale. To achieve optimum hardness, Young's modulus, thermal conductivity, and wear resistance, future experiments should concentrate on the optimization of the nanocarbon concentrations on C-MMCs with improved manufacturing techniques. Future development and improvement can also include further exploration of hybrid metal/carbon and polymer/carbon as reinforcements in MMCs. Nano-, micro-, and macro-tests should also be performed for comparison purposes to validate the reinforcement-matrix interaction at the interface.

ACKNOWLEDGEMENTS

The authors acknowledge support from the new faculty startup fund and Materials Technology Center at Southern Illinois University (SIUC). This work is partially supported by NSF ERI grant #2138459.

CONFLICT OF INTEREST

On behalf of all the authors, the corresponding author states that there is no conflict of interest.

REFERENCES

- A. Taub, E. De Moor, A. Luo, D.K. Matlock, J.G. Speer, and U. Vaidya, Annu. Rev. Mater. Res. 49, 327 (2019).
- S.R. Bakshi, D. Lahiri, and A. Agarwal, Int. Mater. Rev. 55,
- H.H. Chen, W.L. Ma, Z.Y. Huang, Y. Zhang, Y. Huang, and Y.S. Chen, Adv. Opt. Mater. 7, 1801318 (2019).
- J.A. Ali, A.M. Kalhury, A.N. Sabir, R.N. Ahmed, N.H. Ali, and A.D. Abdullah, J. Pet. Sci. Eng. 191, 107118 (2020).
- Z. Hu, G. Tong, D. Lin, C. Chen, H. Guo, J. Xu, and L. Zhou, Mater. Sci. Technol. 32, 930 (2016).
- M. Tabandeh-Khorshid, A. Kumar, E. Omrani, C. Kim, and P. Rohatgi, Compos. B. Eng. 183, 107664 (2020).
- C.J. Nicholls, B. Boswell, I.J. Davies, and M.N. Islam, Int. J. Adv. Manuf. Technol. 90, 2429 (2017).
- E. Ghasali, M. Alizadeh, M. Niazmand, and T. Ebadzadeh, J. Alloys Compd. 697, 200 (2017).
- A. Mortensen, and J. Llorca, Annu. Rev. Mater. Res. 40, 243
- U.R. Kanth, P.S. Rao, and M.G. Krishna, J. Mater. Res. Technol. 8, 737 (2019).
- M. Imran, and A.R.A. Khan, J. Mater. Res. Technol. 8, 3347
- C. Ayyappadas, A. Muthuchamy, A.R. Annamalai, and D.K. Agrawal, Adv. Powder Technol. 28, 1760 (2017)
- M. Shukla, S.K. Dhakad, P. Agarwal, and M.K. Pradhan, Mater. Today Proc. 5, 5830 (2018).
- K. Shirvanimoghaddam, S.U. Hamim, M.K. Akbari, S.M. Fakhrhoseini, H. Khayyam, A.H. Pakseresht, E. Ghasali, M. Zabet, K.S. Munir, S.A. Jia, J.P. Davim, and M. Naebe, Compos. Part A: Appl. Sci. Manuf. 92, 70 (2017). Q. Guo, K. Kondoh, and S.M. Han, MRS Bull. 44, 40 (2019).
- A. Naseer, F. Ahmad, M. Aslam, B.H. Guan, W.S.W. Harun, N. Muhamad, M.R. Raza, and R.M. German, Mater. Manuf. Process. 34, 957 (2019).

- 17. X.H. Qu, L. Zhang, M. Wu, and S.B. Ren, Prog. Natl. Sci. Mater. 21, 189 (2011).
- 18. B. Previtali, D. Pocci, and C. Taccardo, Compos. Part A: Appl. Sci. Manuf. 39, 1606 (2008). W.L. Yang, L.P. Zhou, K. Peng, J.J. Zhu, and L. Wan,
- Compos. B. Eng. 55, 1 (2013).
- 20. H. Ghodrati, and R. Ghomashchi, Flatchem 16, 100113
- 21. F. Ogawa, and C. Masuda, Mater. Sci. Eng. A Struct. 820, 141542 (2021).
- S.S. Li, Y.S. Su, Q.B. Ouyang, and D. Zhang, Mater. Lett. 167, 118 (2016).
- M. Bakir, and I. Jasiuk, Adv. Mater. Lett. 8, 105185 (2017).
- 24. L.L. Dong, Y.Q. Fu, Y. Liu, J.W. Lu, W. Zhang, W.T. Huo, L.H. Jin, and Y.S. Zhang, Carbon 173, 41 (2021).
- Y.H.G. Sasaki, Z. Xu, K. Sugio, H. Fukushima, Y. Choi, and K. Matsugi, Mater. Sci. Forum 654-656, 2692 (2010).
- C.F. Deng, D.Z. Wang, X.X. Zhang, and A.B. Li, Mater. Sci. Eng. A Struct. 444, 138 (2007).
- Z. Zhao, P. Bai, W. Du, B. Liu, D. Pan, R. Das, C. Liu, and Z. Guo, Carbon 170, 302 (2020).
- H. Wang, Z.H. Zhang, H.M. Zhang, Z.Y. Hu, S.L. Li, and X.W. Cheng, Mater. Sci. Eng. A Struct. 696, 80 (2017).
- P. Maurya, N. Kota, J. Gibmeier, A. Wanner, and R. Sid-
- dhartha, *Mater. Sci. Eng. A Struct.* 840, 142973 (2022). Z.B. Qi, P. Sun, F.P. Zhu, Z.C. Wang, D.L. Peng, and C.H. Wu, Surf. Coat. Technol. 205, 3692 (2011).
- C.B.A.D. Apelian, Mater. Sci. Forum 678, 1 (2011).
- www.webofknowledge.com, in (2022).
- M.M. Titirici, R.J. White, N. Brun, V.L. Budarin, D.S. Su, F. del Monte, J.H. Clark, and M.J. MacLachlan, Chem. Soc. Rev. 44, 250 (2015).
- O.A. Williams, Diam. Relat. Mater. 20, 621 (2011).
- E.H.L. Falcao, and F. Wudl, J. Chem. Technol. Biotechnol. 82, 524 (2007)
- S.K. Tiwari, V. Kumar, A. Huczko, R. Oraon, A. De Adhikari, and G.C. Nayak, Crit. Rev. Solid State Mater. Sci. 41, 257 (2016).
- C. Thilgen, and F. Diederich, Chem. Rev. 106, 5049 (2006).
- J. Prasek, J. Drbohlavova, J. Chomoucka, J. Hubalek, O. Jasek, V. Adam, and R. Kizek, J. Mater. Chem. 21, 15872 (2011).
- D.L.S. Bakshi, R. Patel, and A. Argarwal, Thin Solid Films 518, 1703 (2010).
- S. Iijima, Nature 354, 56 (1991).
- R. George, K.T. Kashyap, R. Raw, and S. Yamdagni, Scr. Mater. 53, 1159 (2005).
- F. Gao, J.M. Qu, and M. Yao, J. Appl. Phys. 110, 124314
- J.A. Hu, Q.M. Gao, Y.H. Wu, and S.Q. Song, Int. J. Hydrog. Energy 32, 1943 (2007).
- C.T. Kingston, and B. Simard, Anal. Lett. 36, 3119 (2003).
- 45. M. Dienwiebel, G.S. Verhoeven, N. Pradeep, J.W.M. Frenken, J.A. Heimberg, and H.W. Zandbergen, Phys. Rev. Lett. 92, 126101 (2004).
- 46. M. Inagaki, Y. Yang, and F.Y. Kang, Adv. Mater. 24, 2547 (2012).
- H.G.P. Kumar, and M.A. Xavior, Procedia Eng. 97, 1033 (2014).
- M.Z. Cai, D. Thorpe, D.H. Adamson, and H.C. Schniepp, J.
- Mater. Chem. 22, 24992 (2012). 49. X. Li, J.G. Yu, S. Wageh, A.A. Al-Ghamdi, and J. Xie, Small 12, 6640 (2016).
- Y.Y. Shao, J. Wang, H. Wu, J. Liu, I.A. Aksay, and Y.H. Lin, Electroanalysis 22, 1027 (2010).
- Y.H. Zhang, K.Y. Rhee, D. Hui, and S.J. Park, Compos. B. Eng. 143, 19 (2018).
- M. Chipaux, K.J. van der Laan, S.R. Hemelaar, M. Hasani, T.T. Zheng, and R. Schirhagl, Small 14, 1704263 (2018).
- P. Zhu, P.P. Wang, P.Z. Shao, X. Lin, Z.Y. Xiu, Q. Zhang, E. Kobayashi, and G.H. Wu, Int. J. Min. Met. Mater. 29, 200
- S. Kumar, M. Nehra, D. Kedia, N. Dilbaghi, K. Tankeshwar, and K.H. Kim, Carbon 143, 678 (2019).

- M. Amsler, J.A. Flores-Livas, L. Lehtovaara, F. Balima, S.A. Ghasemi, D. Machon, S. Pailhes, A. Willand, D. Caliste, S. Botti, A. San Miguel, S. Goedecker, and M.A.L. Marques, *Phys. Rev. Lett.* 108, 065501 (2012).
- A.D. Jara, A. Betemariam, G. Woldetinsae, and J.Y. Kim, Int. J. Min. Sci. Technol. 29, 671 (2019).
- Y. Li, Y.X. Lu, P. Adelhelm, M.M. Titirici, and Y.S. Hu, *Chem. Soc. Rev.* 48, 4655 (2019).
- M. Terrones, A.R. Botello-Mendez, J. Campos-Delgado, F. Lopez-Urias, Y.I. Vega-Cantu, F.J. Rodriguez-Macias, A.L. Elias, E. Munoz-Sandoval, A.G. Cano-Marquez, J.C. Charlier, and H. Terrones, Nano Today 5, 351 (2010).
- 59. D.D.L. Chung, J. Mater. Sci. 37, 1475 (2002).
- M.S.A. Bhuyan, M.N. Uddin, M.M. Islam, F.A. Bipasha, and S.S. Hossain, *Int. Nano Lett.* 6, 65 (2016).
- D.J. Woo, F.C. Heer, L.N. Brewer, J.P. Hooper, and S. Osswald, *Carbon* 86, 15 (2015).
- S. Yin, Y. Xie, J. Cizek, E.J. Ekoi, T. Hussain, D.P. Dowling, and R. Lupoi, *Compos. B. Eng.* 113, 44 (2017).
- B. Mukherjee, O.S. Asiq Rahman, A. Islam, M. Sribalaji, and A.K. Keshri, J. Alloys Compd. 727, 658 (2017).
- P.S. Bains, S.S. Sidhu, and H.S. Payal, *Mater. Manuf. Process.* 31, 553 (2016).
- X. Ge, C. Klingshirn, M. Wuttig, K. Gaskell, P. Zavalij, Y. Liang, C. Shumeyko, D. Cole, and L. Salamanca-Riba, Carbon 149, 203 (2019).
- B. Ma, U. Balachandran, J. Wang, J. Wen, T.H. Lee, S.E. Dorris, and A.J. Rondinone, Appl. Phys. Lett. 113, 173102 (2018).
- K. Ravi-Kumar, K. Kiran, and V.S. Sreebalaji, *J. Alloys Compd.* 723, 795 (2017).
- R. Arunachalam, P.K. Krishnan, and R. Muraliraja, J. Manuf. Process. 42, 213 (2019).
- B. Chen, S.F. Li, H. Imai, L. Jia, J. Umeda, M. Takahashi, and K. Kondoh, Compos. Sci. Technol. 113, 1 (2015).
- L.G. Hou, R.Z. Wu, X.D. Wang, J.H. Zhang, M.L. Zhang, A.P. Dong, and B.D. Sun, J. Alloys Compd. 695, 2820 (2017)
- F.-C. Wang, Z.-H. Zhang, Y.-J. Sun, Y. Liu, Z.-Y. Hu, H. Wang, A.V. Korznikov, E. Korznikova, Z.-F. Liu, and S. Osamu, Carbon 95, 396 (2015).
- W.-M. Tian, S.-M. Li, B. Wang, X. Chen, J.-H. Liu, and M. Yu, Int. J. Miner. Metall. 23, 723 (2016).
- S.E. Shin, Y.J. Ko, and D.H. Bae, Compos. B. Eng. 106, 66 (2016)
- 74. S. Zhao, Z. Zheng, Z.X. Huang, S.J. Dong, P. Luo, Z. Zhang, and Y.W. Wang, *Mater. Sci. Eng. A Struct.* 675, 82 (2016).
- X. Zhang, C.S. Shi, E.Z. Liu, F. He, L.Y. Ma, Q.Y. Li, J.J. Li, W. Bacsa, N.Q. Zhao, and C.N. He, *Nanoscale* 9, 11929 (2017).
- A.T. Miranda, L. Bolzoni, N. Barekar, Y. Huang, J. Shin,
 S.-H. Ko, and B.J. McKay, *Mater. Des.* 156, 329 (2018).
- L. Chen, Z. Hou, Y. Liu, C. Luan, L. Zhu, and W. Li, *Compos. Part A: Appl. Sci. Manuf.* 138, 106063 (2020).
- C.B. Lin, Z.C. Chang, Y.H. Tung, and Y.Y. Ko, Wear 270, 382 (2011).
- F.Y. Chen, J.M. Ying, Y.F. Wang, S.Y. Du, Z.P. Liu, and Q. Huang, *Carbon* 96, 836 (2016).
- T. Wen, K. Fan, and F. Zhang, J. Alloys Compd. 814, 152303 (2020).
- Z. Cao, X.D. Wang, J.L. Li, Y. Wu, H.P. Zhang, J.Q. Guo, and S.Q. Wang, J. Alloys Compd. 696, 498 (2017).
- C.D. Li, X.J. Wang, W.Q. Liu, K. Wu, H.L. Shi, C. Ding, X.S. Hu, and M.Y. Zheng, *Mater. Sci. Eng. A: Struct.* 597, 264 (2014).
- H. Li, X. Dai, L. Zhao, B. Li, H. Wang, C. Liang, and J. Fan, J. Alloys Compd. 785, 146 (2019).
- J.Y. Hwang, B.K. Lim, J. Tiley, R. Banerjee, and S.H. Hong, Carbon 57, 282 (2013).
- T.P.D. Rajan, and B.C. Pai, Mater. Sci. Forum 690, 157 (2011).
- H. Uozumi, K. Kobayashi, K. Nakanishi, T. Matsunaga, K. Shinozaki, H. Sakamoto, T. Tsukada, C. Masuda, and M. Yoshida, *Mater. Sci. Eng. A: Struct.* 495, 282 (2008).

- 87. F. Wu, and J. Zhu, Compos. Sci. Technol. 57, 661 (1997).
- M. Sanchez, J. Rams, and A. Urena, Compos. Part A: Appl. Sci. Manuf. 41, 1605 (2010).
- H.A. Alhashmy, and M. Nganbe, *Mater. Des.* 67, 154 (2015).
- R. Etemadi, B. Wang, K.M. Pillai, B. Niroumand, E. Omrani, and P. Rohatgi, *Mater. Manuf. Process.* 33, 1261 (2018).
- Z.Y. Liu, B.L. Xiao, W.G. Wang, and Z.Y. Ma, Compos. Part A. Appl. Sci. Manuf. 94, 189 (2017).
- K.S. Munir, Y.F. Zheng, D.L. Zhang, J.X. Lin, Y.C. Li, and C.E. Wen, *Mater. Sci. Eng. A: Struct.* 696, 10 (2017).
- S. Simoes, F. Viana, M.A.L. Reis, and M.F. Vieira, *Metals* 7, 279 (2017).
- H. Deng, J.H. Yi, C. Xia, and Y. Yi, J. Alloys Compd. 727, 260 (2017).
- Z.H. Yu, W.S. Yang, C. Zhou, N.B. Zhang, Z.L. Chao, H. Liu, Y.F. Cao, Y. Sun, P.Z. Shao, and G.H. Wu, *Carbon* 141, 25 (2019).
- K.S. Munir, Y.C. Li, M. Qian, and C. Wen, Carbon 99, 384 (2016).
- Z.Y. Liu, S.J. Xu, B.L. Xiao, P. Xue, W.G. Wang, and Z.Y.
 Ma, Compos. Part A: Appl. Sci. Manuf. 43, 2161 (2012).
- C.R. Bradbury, J.K. Gomon, L. Kollo, H. Kwon, and M. Leparoux, J. Alloys Compd. 585, 362 (2014).
- B. Lasio, F. Torre, R. Orru, G. Cao, M. Cabibbo, and F. Delogu, Mater. Lett. 230, 199 (2018).
- K. Aristizabal, A. Katzensteiner, A. Bachmaier, F. Mucklich, and S. Suarez, *Mater. Charact.* 136, 375 (2018).
- N. Chamroune, D. Mereib, F. Delange, N. Caillault, Y.F. Lu, J.L. Grosseau-Poussard, and J.F. Silvain, J. Mater. Sci. 53, 8180 (2018).
- I. Carneiro, F. Viana, M.F. Vieira, J.V. Fernandes, and S. Simoes, Nanomaterials 9, 878 (2019).
- N.Y. Li, C. Yang, C.J. Li, H.D. Guan, D. Fang, J.M. Tao,
 Y.C. Liu, and J.H. Yi, *Diam. Relat. Mater.* 107, 107907 (2020).
- B. Sadeghi, P. Cavaliere, G.A. Roeen, M. Nosko, M. Shamanian, V. Trembosova, S. Nagy, and N. Ebrahimzadeh, Adv. Compos. Hybrid. Mater. 2, 549 (2019).
- M. Jagannatham, P. Chandran, S. Sankaran, P. Haridoss, N. Nayan, and S.R. Bakshi, Carbon 160, 14 (2020).
- K.S. Munir, P. Kingshott, and C. Wen, Crit. Rev. Solid State Mater. Sci. 40, 38 (2015).
- H.J. Ling, Y.J. Mai, S.L. Li, L.Y. Zhang, C.S. Liu, and X.H. Jie, Surf. Coat. Technol. 364, 256 (2019).
- S.R. Bakshi, V. Singh, S. Seal, and A. Agarwal, Surf. Coat. Technol. 203, 1544 (2009).
- L.W. He, and M. Hassani, J. Therm. Spray Technol. 29, 1565 (2020).
- X.L. Xie, S. Yin, R.N. Raoelison, C.Y. Chen, C. Verdy, W.Y. Li, G. Ji, Z.M. Ren, and H.L. Liao, *J. Mater. Sci. Technol.* 86, 20 (2021).
- M.Q. Kareem, A.H. Jasim, and N.A.-A. Hamza, Open Eng. 10, 1 (2020).
- M.L.B. Peng, P. Zapol, S.Y. Li, S.I. Mielke, G.C. Schatz, and H.D. Espinosa, Nat. Nanotechnol. 3, 626 (2008).
- P. Samal, P.R. Vundavilli, A. Meher, and M.M. Mahapatra, J. Manuf. Process. 59, 131 (2020).
- D. Wu, W.Y. Li, K. Liu, Y. Yang, and S.J. Hao, J. Mater. Sci. Technol. 106, 211 (2022).
- S.N. Alam, and L. Kumar, Mater. Sci. Eng. A Struct. 667, 16 (2016).
- S.B.Y. Chen, and A. Agarwal, Surf. Coat. Technol. 204, 2709 (2010).
- P. Garg, A. Jamwal, D. Kumar, K.K. Sadasivuni, C.M. Hussain, and P. Gupta, J. Mater. Res. Technol. 8, 4924 (2019).
- 118. A.V. Radhamani, H.C. Lau, and S. Ramakrishna, Compos. Part A: Appl. Sci. Manuf. 114, 170 (2018).
- B. Chen, K. Kondoh, H. Imai, J. Umeda, and M. Takahashi, Scr. Mater. 113, 158 (2016).
- 120. W.W. Zhou, S. Bang, H. Kurita, T. Miyazaki, Y. Fan, and A. Kawasaki, *Carbon* 96, 919 (2016).

- H. Hanizam, M.S. Salleh, M.Z. Omar, and A. Sulong, J. Mater. Res. Technol. 8, 2223 (2019).
- C. Isaza, G. Sierra, and J.M. Meza, J. Manuf. Sci. Eng. 138, 024501 (2016).
- P. Hidalgo-Manrique, X.Z. Lei, R.Y. Xu, M.Y. Zhou, I.A. Kinloch, and R.J. Young, *J. Mater. Sci.* 54, 12236 (2019).
- S. Ali, F. Ahmad, P.S.M.M. Yusoff, N. Muhamad, E. Onate, M.R. Raza, and K. Malik, *Compos. Part A: Appl. Sci. Manuf.* 144, 106357 (2021).
- S. Cho, K. Kikuchi, T. Miyazaki, K. Takagi, A. Kawasaki, and T. Tsukada, Scr. Mater. 63, 375 (2010).
- J.T.S. Dong, and X. Zhang, Mater. Sci. Eng. A 313, 83 (2001).
- K.K.S. Cha, S. Arshad, C. Mo, and S. Hong, Adv. Mater. 17, 1377 (2005).
- X. Zhang, Y.X. Xu, M.C. Wang, E.Z. Liu, N.Q. Zhao, C.S. Shi, D. Lin, F.L. Zhu, and C.N. He, *Nat. Commun.* 11, 2775 (2020).
- X. Zhang, C.S. Shi, E.Z. Liu, N.Q. Zhao, and C.N. He, ACS Appl. Mater. Inter. 10, 37586 (2018).
- H.J. Cho, D. Yan, J. Tam, and U. Erb, J. Alloys Compd. 791, 1128 (2019).
- V.D.P. Martis, J. Delhalle, and Z. Mekhalif, *Electrochim. Acta* 55, 5407 (2010).
- 132. X.C.H. Chai, D. Jia, and W. Zhou, Rare Met. 30, 85 (2011).
- 133. T.B.A.S. Harimkar, Surf. Eng. 27, 524 (2011).
- 134. P.S.C. Carpenter, and Y. Zhu, Wear 271, 2100 (2011).
- R.G.S. Yamanaka, A. Kawasaki, H. Sakamoto, Y. Mekuchi, M. Kuno, and T. Tsukada, *Mater. Trans.* 48, 2506 (2007).
- M.A.S. Mirzamohammadi, A. Sabur, and A. Hassanzadeh-Tabrizi, Mater. Sci. 46, 1 (2010).
- 137. J.Q.F. Gao, and M. Yao, J. Appl. Phys. 110, 124314 (2011).
- Y. Sun, J.R. Sun, M. Liu, and Q.F. Chen, *Nanotechnology* 18, 505704 (2007).
- 139. H.W.Y. Jeng, and P. Tsai, *Diam. Relat. Mater.* 18, 528 (2009).
- 140. A.S.D.P. Sahoo, Mater. Des. 32, 1760 (2011).
- S. Wang, X. Zou, T. Shi, K. Ding, Z. Pang, Y. Huang, W. Tang, Q. Xu, Z. Zhou, and X. Lu, *Appl. Surf. Sci.* 498, 143768 (2019).
- S. Suarez, L. Reinert, M. Zeiger, P. Miska, S. Grandthyll,
 F. Muller, V. Presser, and F. Muklich, Carbon 129, 631 (2018).
- 143. Y. Lei, J.L. Jiang, T.T. Bi, J.F. Du, and X.J. Pang, RSC Adv. 8, 22113 (2018).
- K. Aristizabal, A. Katzensteiner, M. Leoni, F. Mucklich, and S. Suarez, *Mater. Charact.* 154, 344 (2019).

- V.K.D. Chakravarthi, R. Vaidyanathan, J. Blaine, S. Yarlagadda, D. Roseman, Q. Zeng, and E. Barrera, Adv. Funct. Mater. 21, 2527 (2011).
- R.Y.Q. Jiang, G. Fu, D. Xie, B. Huang, Z. He, and Y. Zhao, *Mater. Sci. Forum* 687, 158 (2011).
- 147. S.L.A.S. Park, Adv. Mater. Res. 123–125, 695 (2010).
- Y.C. Fan, Y.M. Liu, Y.C. Chen, Y. Sung, and M.D. Ger, *Appl. Surf. Sci.* 255, 7753 (2009).
- 149. A.Y.L.C. Hsieh, J. Power Sources 188, 347 (2009).
- D.A.S. Noel, F. House, A. Benedetto, P. Viel, S. Palacin, N. Izard, and P. Chenevier, *IEEE Trans. Comp. Packag. Technol.* 32, 358 (2009).
- M.A.J. Siqueira, M. Backer, V. Zucolotto, A. Poghossian, O. Oliveira, and M. Schoning, PSS (A) 206, 462 (2009).
- S. Abazari, A. Shamsipur, H.R. Bakhsheshi-Rad, A.F. Ismail, S. Sharif, M. Razzaghi, S. Ramakrishna, and F. Berto, *Materials* 13, 4421 (2020).
- S.L. Xiang, X.J. Wang, M. Gupta, K. Wu, X.S. Hu, and M.Y. Zheng, Sci. Rep. 6, 38824 (2016).
- H.S. Abdo, K.A. Khalil, M.M. El-Rayes, W.W. Marzouk, A.-F.M. Hashem, and G.T. Abdel-Jaber, J. King Saud. Univ. Eng. Sci. 32, 346 (2020).
- 155. X.N. Mu, H.N. Cai, H.M. Zhang, Q.B. Fan, F.C. Wang, Z.H. Zhang, Y.X. Ge, R. Shi, Y. Wu, Z. Wang, D.D. Wang, and S. Chang, *Carbon* 137, 146 (2018).
- M.D. Hayat, H. Singh, Z. He, and P. Cao, Compos. Part A: Appl. Sci. Manuf. 121, 418 (2019).
- T.T.K. Kondoh, H. Imai, J. Umeda, and B. Fugetsu, Compos. Sci. Technol. 69, 1077 (2009).
- 158. E.N.I. Melendez, P. Angerer, H. Danninger, and J. Torralba, Compos. Sci. Technol. 71, 1154 (2011).
- J.S.K. He, D. Guo, Y. Xing, and G. Zhang, PSS (A) 208, 2388 (2011).
- 160. Y.Z.J. Lv, and H. Zhao, Synth. Mater. 160, 2051 (2010).

Publisher's Note Springer Nature remains neutral with regard to jurisdictional claims in published maps and institutional affiliations.

Springer Nature or its licensor (e.g. a society or other partner) holds exclusive rights to this article under a publishing agreement with the author(s) or other rightsholder(s); author self-archiving of the accepted manuscript version of this article is solely governed by the terms of such publishing agreement and applicable law.